State-of-the-Art Neoclassical Tearing Mode Control in DIII-D Using Real-time Steerable Electron Cyclotron Current Drive Launchers

E. Kolemen[1], A.S. Welander[2], R.J. La Haye[2], N.W. Eidietis[2], D.A. Humphreys[2], J. Lohr[2], V. Noraky[2], B.G. Penaflor[2], R. Prater[2], and F. Turco[3]

[1]*Princeton Plasma Physics Laboratory, Princeton, NJ 08543-0451, USA*

[2]*General Atomics, PO Box 85608, San Diego, CA 92186-5608, USA*

[3]*Columbia University, 116th St and Broadway, New York, NY 10027, USA*

Abstract: Real time steerable electron cyclotron current drive (ECCD) has been demonstrated to reduce the power requirements and time needed to remove 3/2 and 2/1 neoclassical tearing modes (NTM) in the DIII-D tokamak. In a world first demonstration of the techniques required in ITER, the island formation onset is detected automatically, gyrotrons are turned on and the real-time steerable ECCD launcher mirrors are moved promptly to drive current at the location of the islands. This shrinks and suppresses the modes well before saturation using real-time motional Stark effect (MSE) constrained equilibria reconstruction with advanced feedback and search algorithms to target the deposition. In ITER, this method will reduce the ECCD energy requirement and so raise Q by keeping the EC system off when the NTM is not present. Further, in the experiments with accurate tracking of pre-emptive ECCD to resonant surfaces, both 3/2 and 2/1 modes are prevented from appearing with much lower ECCD peak power than required for removal of a saturated mode.

PACS Numbers: 52.35.Py, 52.55.Fa, 52.55.Wq, and 52.35.Hr

1. Introduction

The tearing mode is an MHD instability that is caused by a perturbation to the plasma current, which generates a magnetic island on a rational flux surface. The NTM is a metastable tearing mode, which is classically stable but can be destabilized by a helical perturbation of the bootstrap current. Fully grown NTMs with poloidal mode/toroidal mode m/n=3/2 degrade the energy confinement by typically 10%–30%, while modes with m/n=2/1 lead to severe energy loss and frequently to disruption [1].

Microwave powered co-current drive at the mode rational surface can suppress the NTM by increasing the linear stability and replacing the missing bootstrap current. Electrons gyrate around magnetic field lines as they travel in the toroidal direction. A microwave beam at the electron cyclotron resonant frequency will deposit energy into the electrons. The ECCD is obtained by finite parallel refractive index, $n_{||}$, by oblique injection to the magnetic field. There are many ways of producing current drive in tokamaks, but for NTM control, ECCD has the advantages of narrow current drive placed at a specific harmonic cyclotron resonance, scalable high power and long pulse operation [2]. A crucial step in NTM control with ECCD is the alignment of the ECCD with the NTM.

The use of ECCD for NTM control has been studied in various tokamaks including ASDEX Upgrade [11], DIII-D [2], TEXTOR [12], Tore Supra [13], JT-60U [14,15,16]. In DIII-D, successful NTM stabilization has been achieved, and it has been shown that preemptive stabilization of NTMs by application of highly localized ECCD has led to operation at increased plasma pressure, up to the no-wall kink limit [2]. In previous experiments at DIII-D, ECCD deposition locations (ECCD current density profile) were changed by moving the plasma in and out radially (NTM island moved with respect to the $2f_{ce}$ resonance) or by changing the toroidal field and thus the $2f_{ce}$ resonance location [2,3].

However, these methods change the plasma equilibrium, and thus resulted in minimal use in regular physics experiments. Consequently, a new real-time ECCD launcher mirror control system was installed in 2012 as part of a major NTM control upgrade. This allowed alignment of ECCD with the NTM by moving the mirrors while keeping the plasma conditions fixed.

Details of the new NTM control system in DIII-D and its application are described in this paper. In the introduction, we first examine the significance of ITER NTM control. Then, the current NTM control strategies using ECCD are discussed. In section two, an overview of the new NTM control system in DIII-D using real-time steerable ECCD launchers is provided. In the third section, a novel control approach to NTM control named the "catch and subdue" with reduced power and time requirement is introduced. The fourth section shows the results of the DIII-D experiments with this new system where the different NTM control approaches are compared. Finally, in the fifth section, the conclusions of the analysis and directions for future work are discussed.

2. The Upgraded DIII-D NTM Control System

Evidence from experimental results and numerical simulations show that without NTM control ITER is likely to have unstable 2/1 islands. Figure 1 shows how the 2/1 island is expected to behave in ITER. Based on the DIII-D experiments designed to mimic ITER conditions and numerical simulations, the ITER 2/1 island is expected to grow in size leading to wall locking and a loss of H-mode and eventually disruption. Thus, there is need for development of robust and efficient NTM control strategies for ITER.

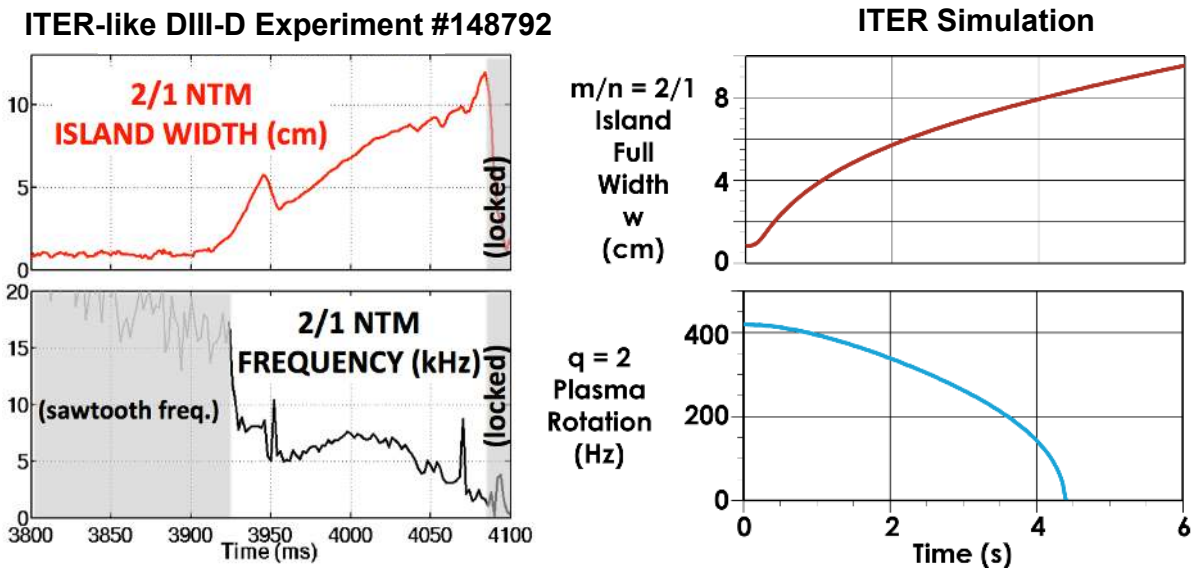

Fig 1. Growth of the 2/1 island and the locking of the mode in ITER: On the left: Experimental result from DIII-D with an ITER-like configuration (Shot #148792). On the right: Numerical simulation of the ITER behavior from Ref. [7].

The architecture of the real-time mirror steering NTM control system in DIII-D is shown in figure 2. An overview of the system is given in this section; see Kolemen et al. [4] for details. The system consists of the diagnostic measurement, Plasma Control System (PCS) logic, and the mirror and gyrotron actuators.

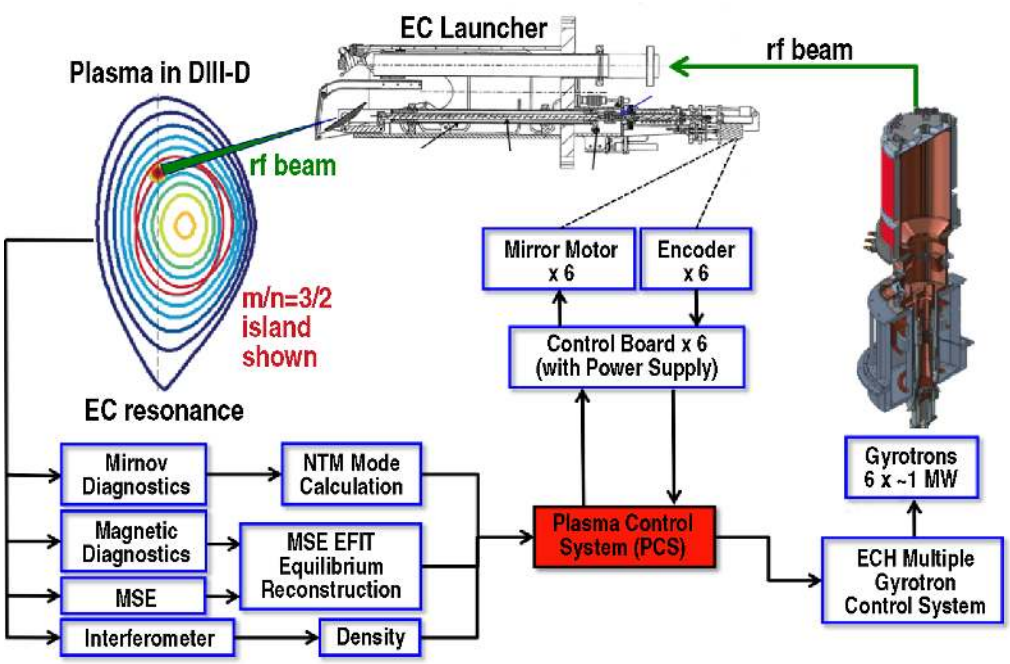

Figure 2. Block diagram of the real-time NTM control system.

DIII-D had six gyrotrons with associated waveguides and EC launcher in the 2012 campaign, five of which were available during the NTM control experiments. This enabled the generation of a microwave beam with a total injected power of ~2.8 MW that can be sustained for up to 5-10 seconds, and directed by the steerable EC launchers [5].

The internal plasma profiles and MHD activity are monitored by a comprehensive set of diagnostics. The real-time NTM control system uses the Mirnov diagnostics for detecting MHD modes, Motional Stark Effect (MSE) diagnostics for current profile reconstruction, magnetic sensors for equilibrium reconstruction and interferometer signals for density measurement. The real-time equilibrium reconstruction is obtained by MSE constrained EFIT. A dedicated computer running real-time Fourier analysis of the Mirnov measurements obtains the n=1,2 mode amplitude, frequency and the phase. The density in the plasma (which can cause refraction of the rf beam) is obtained from the interferometer signals.

This diagnostic information is used by PCS to move the real-time steerable ECH launcher mirrors and direct the ECCD to the NTM location. Similarly, the PCS decides on the

gyrotron power level and sends the request to the ECH Multiple Gyrotron Control System [6].

2.1. Real-time mirror control

For these experiments a new real-time control system was installed for the ECH launcher mirrors this year. This system allows the PCS control using the diagnostic information to move the real-time steerable ECH launcher mirrors and direct the ECCD to the NTM location. The PCS NTM control logic calculates the desired q-surface location corresponding to the NTM mode (3/2, 2/1) from the MSE-EFIT reconstruction. The target for the ECCD is then obtained by the intersection of the q-surface with the $2f_{ce}$ surface. The ECH launch mirror angle that aligns the ECCD with the target is obtained by using a linearized ray tracing algorithm and compensated for the refraction due to changes in the density. The system was extensively calibrated to enable precise ECCD tracking of the calculated resonant surface. The main requirement of the NTM suppression at DIII-D is to keep alignment of the center of the ECCD deposition with respect to the rational surface within 1 cm as discussed in reference [1]. The control system meets this spec by achieving better than 1 cm accuracy as can be seen in figure 3 which shows the calculated z position of the rational surface (black line) and the ECCD deposition center (red line). The ECCD deposition calibration was obtained by modulating the ECCD at 70-100 Hz. The amplitude of the T_e modulation at the EC frequency in the ECE channels was measured. These were then interpolated to find the peak amplitude location that corresponds to the center of the EC deposition location. These results were compared to ray-tracing to calibrate the tracing algorithm. q surface calculations by real time MSE reconstructions were calibrated against the ECE based NTM location calculations. Finally, ECCD was swept across the NTM; it was observed that the maximum

suppression occurred at the location where the algorithm calculated the NTM and the ECCD were in alignment as expected.

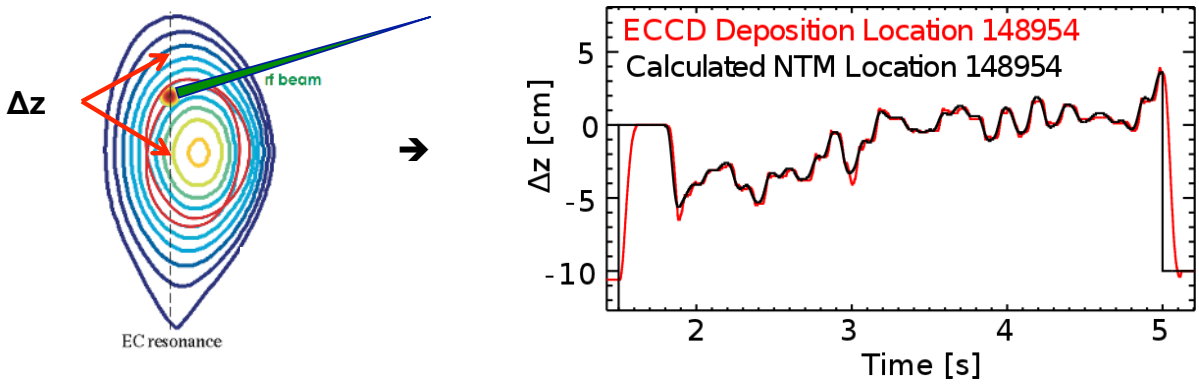

Figure 3. Advanced control of the steerable-mirror enables real-time tracking of the NTM. Δz is the difference between the z position of the intersection of the q-surface with the $2f_{ce}$ surface and the average z-position estimated from similar shots.

3. A Novel NTM Control Approach: "Catch and Subdue"

3.1. Need for a new NTM control approach

Due to fast time scales and non-reproducibility/random nature of the NTM formation, numerical algorithms must decide when to turn on the ECCD deposition and align it with the NTM. NTM control techniques used to date consisted of either preemption (CW ECCD at the mode rational surface to avoid a mode appearing) or suppression of a saturated NTM.

In the saturated NTM suppression, ECCD is turned on after an NTM island saturates, and is aimed at the center of the NTM island. This reduces the size of the island until it is fully suppressed as shown in figure 4 for 3/2 NTM. One problem with this approach to suppression is that it takes a long time for the NTM to be suppressed, if at all; often, the more important issue with this method is that the 2/1 NTM usually does not saturate to a stable size but locks and disrupts before it can be stabilized.

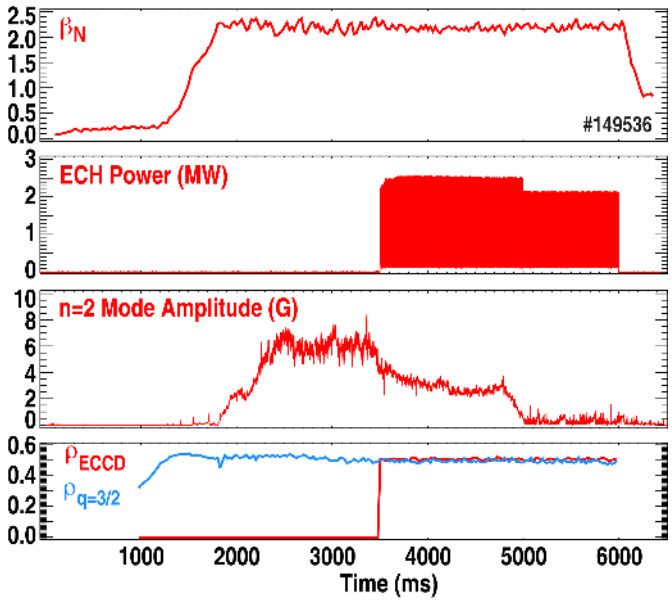

Figure 4. Suppression of a saturated NTM formation by depositing ECCD (slowly modulated for alignment checkout) at the island location after the mode appears.

In the NTM preemption method, the ECCD is turned to drive current at the appropriate rational flux surface before a mode would otherwise appear. This stabilizes the plasma to perturbations that would trigger NTMs. An example of this NTM preemption is shown in figure 5 for a shot with toroidal magnetic field, B_T=1.8 Tesla, plasma current, I_p=1.25 MA, β_N,=2.2, edge safety factor, q_{95}=4.3, and density, n_e=4x10^{19} m^{-3}. Note that in the figure, two modes appear around 2.5 and 3.5 seconds but are quickly damped due to the ECCD suppression. This is the present NTM control method envisioned for ITER.

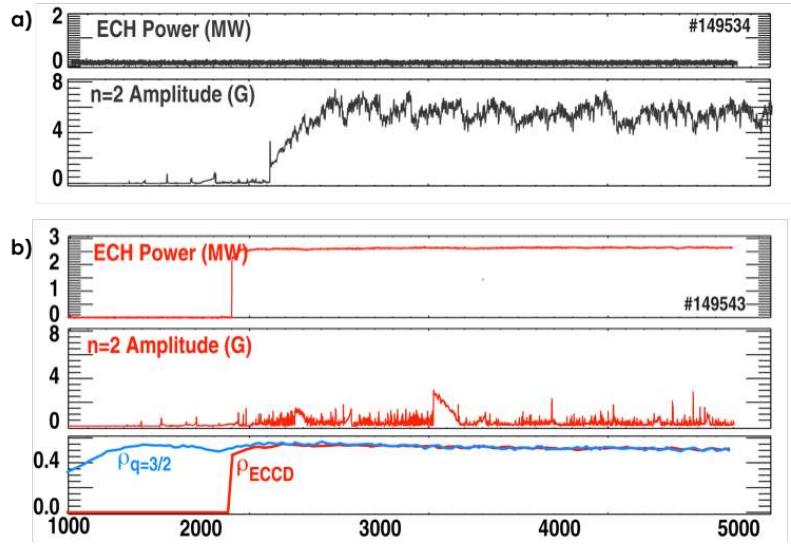

Figure 5. a) Experiment with no ECCD, a 3/2 NTM forms and saturates. b) Repeat of the same experiment with pre-emption of NTM formation by depositing ECCD at the island location before the mode appears. "Incidents" at t ≈ 2500 and 3300 msec. are quickly suppressed automatically.

Both preemptive NTM control and suppression after NTM saturation pose issues as ITER control strategies. Waiting to suppress the mode until it saturates increases the risk of disruption. On the other hand, preemptive suppression uses continuous EC power even if there is no need for it at a given time. This decreases operating fusion energy gain factor, Q, for ITER. The reduction depends on the power required for suppression. The effect of the preemptive EC use for NTM control on the ITER Q performance was studied in [8], which shows that if 7 MW of preemptive EC power is used at ITER, the achievable Q is reduced from 10 to 9, and 20 MW of preemptive EC would reduce the achievable Q further to 7. Thus, it is preferable to have an NTM control strategy that does not use the EC when there is no NTM formation and intercepts the mode as it emerges while the island is still small. The benefit that can be realized from such an approach depends on the required duty cycle to keep

the mode under control, which in turn depends on how frequently the modes are triggered and how long it takes for the mode to be suppressed.

3.2. The Catch and Subdue algorithm

A novel NTM control algorithm that automatically detects and suppresses the NTM before full saturation, referred to as "catch and subdue", was developed in these studies. This rapid method allows gyrotrons to be powered off when not needed, thus saving energy as well as maintaining the plasma in a stable condition. The main challenge of this approach is that the island saturation is a fast process taking approximately 100 to 150 ms for the 2/1 mode and 200 ms for the 3/2 mode at DIII-D. Thus, a fast real-time control system was developed for DIII-D, as discussed in Kolemen et al. [4], to replace the older system which did not have real-time positioning capability (no real-time communication with PCS and >100 ms response delay). The new system has a delay of approximately 2 ms and 4-12 ms startup time to overcome static friction at zero velocity.

In this approach, the PCS continuously calculates the q-surface location of the NTM of interest and the ECH launcher mirrors move to track the q-surface, keeping the system ready to suppress at any time. Real-time Fourier analysis of the Mirnov measurements is used to obtain the mode amplitude. When a preset Mirnov amplitude level is exceeded for a predetermined period of time, indicating the presence of an island, the gyrotrons are turned on. The trigger level and the minimum period are adjusted empirically to reduce the false positives but keep the detection time to a minimum. For example for the 2/1 mode, the threshold is set to 7 Gauss and the period to 5 ms. When the mode is detected, the gyrotrons are turned on. Since the mirrors have been tracking the NTM location, instant alignment of the ECCD and NTM is obtained.

An example of catch and subdue suppression is shown in figure 6. The continual mirror alignment enables fast mode suppression (~140 ms after the gyrotrons turn on) before mode

saturation. In the figure, a 5 ms spike in gyrotron power is visible when the control system is turned on at approximately 2 seconds. This full power initialization is necessary for optimal gyrotron operations. Due to technical limitations on the gyrotron power control, a zero power request from the PCS cannot be achieved, and is instead converted to several hundred kilowatts of power. Further, in 2012 NTM experiments, the gyrotron power was not turned off after the mode disappeared. Control algorithm upgrades that will enable this feature are currently developed and ready. After the gyrotrons are turned off in figure 6, the mode does not come back possibly due to formation of a 4/3 island, which preempts the formation of lower order islands.

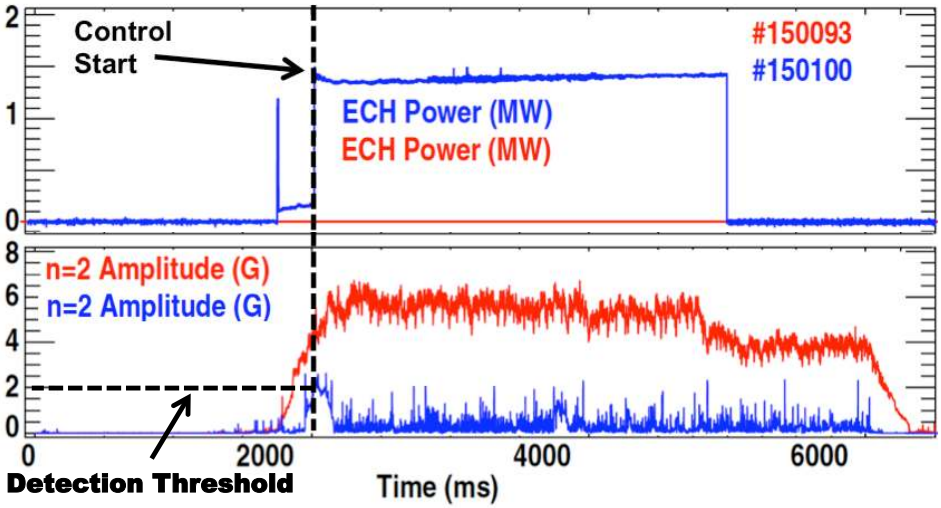

Figure 6. n=2 amplitude (a proxy for 3/2 island size) and the ECCD power for two shots with and without catch and subdue control. In red: Saturated NTM with no ECCD (Beam drops after 5 sec). In blue: Catch and subdue NTM suppression. The ECCD is turned full on when the mode is detected and the mode is promptly suppressed.

4. Results of the DIII-D NTM Control Experiments

Using the real-time NTM control system, 3/2 and 2/1 islands were suppressed experimentally. Control algorithms that were experimentally tested at DIII-D are: (1) ECCD turned on after mode saturation using constant tracking of the mode location; (2) ECCD turned on preemptively driving current at the appropriate rational flux surface before a mode would otherwise appear; (3) "catch and subdue" as described above. The results obtained with these algorithms are compared in this section.

4.1. 3/2 NTM control results

Figure 6 shows 3/2 NTM catch and subdue control for ECCD aligned to the mode rational q surface. Catch and subdue also works well starting from an initially deliberately misaligned ECCD and q surface as shown in figure 7. In the figure, the top three subplots show the mode amplitude, alignment error between the peak ECCD drive and the island, and the ECH power. The onset of the mode, the start of the control after the mode detection and the point at which the mode is stabilized are plotted in dashed lines. All of the above information is combined in the bottom subplot, such that the ρ of the 3/2 surface is shown in white and the extent of the island is shown in the green shaded area against a contour plot of the ECCD current drive, where yellow, red and purple correspond to decreasing values and black corresponds to zero. In this example, the ECCD deposition location is initially deliberately misaligned approximately 4 centimeters high when the algorithm detects the island formation. When the mode is detected, the control automatically fully turns on the gyrotrons and rapidly corrects the deposition location to align with MSE reconstructed q-surface location using real-time motion of the steerable mirrors. It takes less than 0.3 s from the start of the mode growth until its full suppression (0.25 s from control activation). The catch and subdue achieves fast suppression – complete suppression takes only ~40 ms longer

than the aligned case. This result is encouraging for using the gyrotrons for multiple purposes simultaneously. For example, the ECCD can be used for current drive at the core and can be moved to the NTM location when the mode appears and moved back after the suppression.

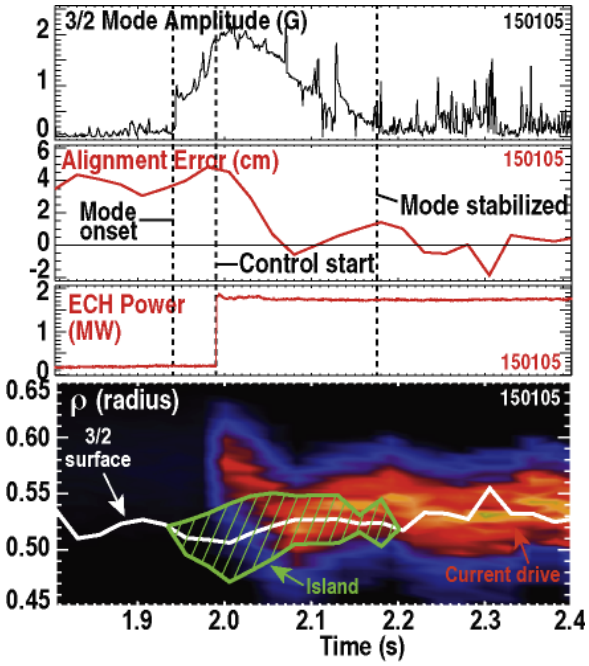

Figure 7. Catch and subdue works well even starting from a deliberate 4 cm misalignment between ECCD and the q surface. *Top:* 3/2 Mode Amplitude. *Top-middle:* Alignment error. *Bottom-middle:* ECH Power. *Bottom:* Contour plot of ECCD current density where black is 0 A/cm^2, blue is 3 A/cm^2, red is 6 A/cm^2, and yellow is 12 A/cm^2. Overlaid in white is the 3/2 surface location and in green is the island size and location.

Contour plots of the achieved mode amplitudes for all the 3/2 NTM control experiments are shown in figure 8. The contour plot is achieved by using each suppression/preemption effort as a single data point (with some discharges, multiple times are taken). For each of these data points, the corresponding EC power for that shot marks the y-axis location and the alignment of the ECCD with the NTM normalized to the full width half maximum (FWHM) of the ECCD current density profile, which is approximately 4-5 cm in the studied shots, marks the x-axis location. The color of the contour z-axis represents the achieved mode

amplitude level at the end of the suppression/preemption effort with magenta corresponding to fully suppressed modes. White space is used when there is no experimental data.

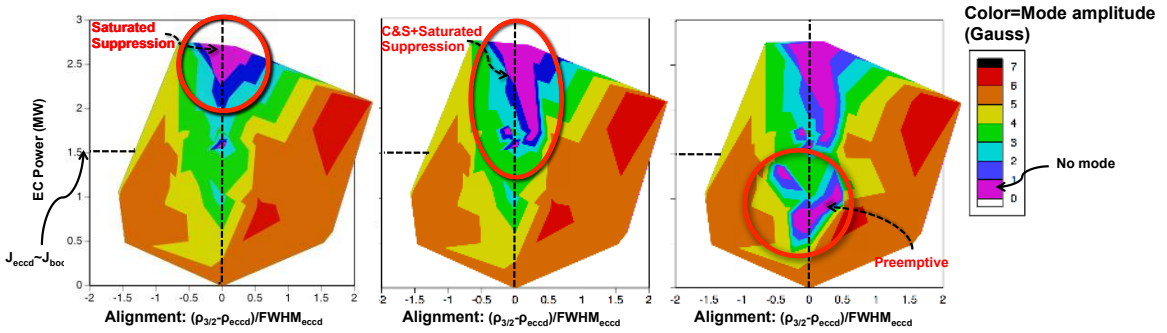

Figure 8. Overview of the 3/2 NTM experiments showing the effects of EC power and its alignment with the q=3/2 surface on magnitude of the mode for different NTM control techniques. Shown in the panel from left to right are the saturated mode suppression, the catch and subdue suppression added, and finally the preemptive suppression added results. In the panels magenta color corresponds to fully suppressed modes.

Successful suppression of saturated 3/2 modes requires good alignment well within half of the width of the ECCD profile and the current drive in the island to be 50% greater than the bootstrap current $\left(J_{eccd} > 1.5 J_{boot}\right)$ [9,10]; this requires significantly greater EC power than "catch and subdue" or preemption. Catch and subdue reduces the necessary power requirement by at least a third compared to saturated mode suppression. However, note that due to experimental time constraints, catch and subdue with lower than 1.5 MW power was not attempted. The lowest EC power to maintain stability, as low as 1/4th of the saturated suppression case, is required if ECCD is applied preemptively and continuously to stop the mode appearing as shown in the overview of the 3/2 results. It is likely that catch and subdue may result in similarly low power requirements as the preemptive suppression. Also, the lowest overall power with preemption is achieved by catching the transiently excited mode while it is small and suppressing it quickly (<0.3 s vs. 1–2 s for fully grown islands).

Early mode detection is a key ingredient for fast mode suppression. Results of an NTM mode detection amplitude threshold scan are shown in figure 9. In the figure, mode size from the start of the automatic detection is plotted for experimental shots (all similar β_N), where the 3/2 mode is detected in real time and ECCD is actively aligned with a power of 1.55 ± 0.2 MW at the island location. In the cases where the mode has been caught at smaller size below the critical amplitude, small island effect takes over and prompt suppression follows. This critical amplitude for the 3/2 island is found to be approximately 2 Gauss, which is equivalent to a full island width of about twice the ion banana width. When the island size at detection increases above the critical level, the mode cannot be suppressed before saturation, and the suppression takes more than a second or may become unachievable during the remainder of the high beta discharge.

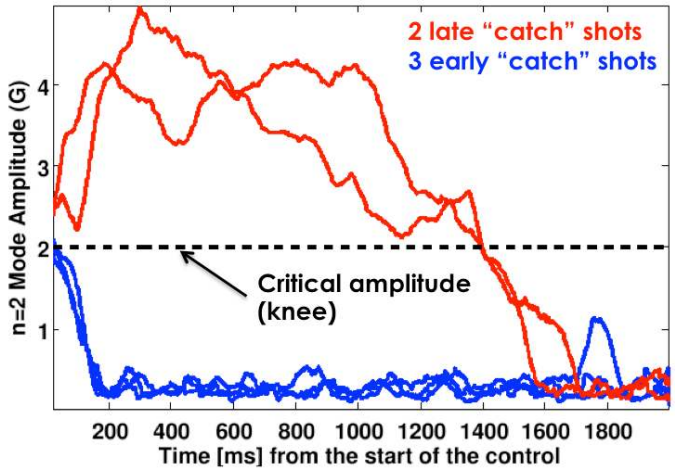

Figure 9. Mode amplitude from the start of the NTM detection and ECCD deposition for 3/2 NTM suppression. In red are 2 late "catch" shots and in blue are the 3 early "catch" shots.

4.2. 2/1 NTM control results

In DIII-D, the 2/1 NTM often leads to rotational locking to the wall in ITER baseline scenarios, with consequent large decreases in performance (loss of H-mode) and possibly disruption. These effects have been avoided using the real-time "catch and subdue" control

system, as shown in figure 10. The mode growth rate is slowed, peak amplitude is reduced (≈40 Gauss for cases without ECCD, not shown here) and the mode is eventually brought to full suppression without locking or loss of H-mode.

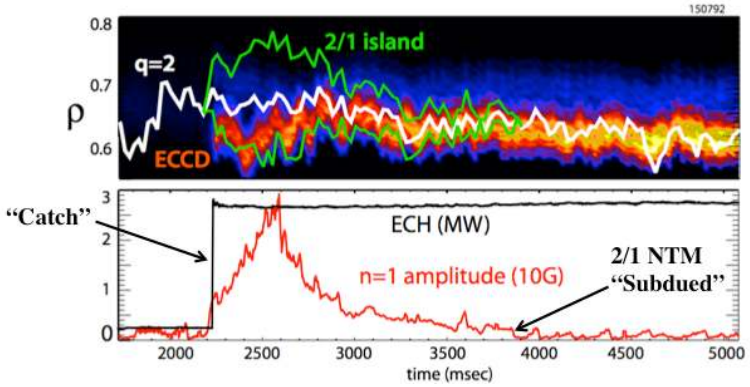

Figure 10. Example of 2/1 "catch and subdue" NTM control. *Top:* 2/1 Mode Amplitude. *Bottom:* Contour plot of ECCD current density where black is 0 A/cm^2, blue is 3 A/cm^2, red is 6 A/cm^2, and yellow is 12 A/cm^2. Overlaid in white is the 2/1 surface location and in green is the island size and location.

Successful 2/1 mode suppression (as for the 3/2 case) requires both good alignment and $J_{eccd} > J_{boot}$ as shown in contour plots in figure 11. This figure shows all the 2/1 mode suppression/preemption attempts from the DIII-D 2012 experimental campaign in the same way as figure 8. In these 2/1 cases, saturated mode suppression is not feasible as locking and beta collapse occur prior to saturation. Note the requirement that $J_{eccd} > J_{boot}$ for catch and subdue suppression of 2/1 pushes the limit of the available EC power of 2.8 MW. Alternatively, in the experiments with accurate tracking of preemptive ECCD to 2/1 resonant surfaces, modes are prevented from appearing with 40% reduced ECCD power requirement.

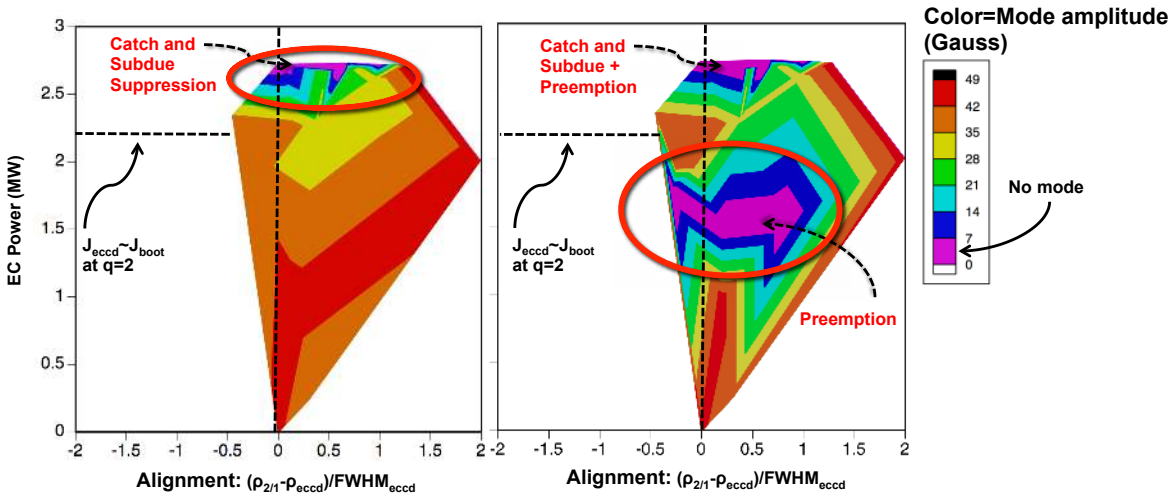

Figure 11. Contour plot overview of the 2/1 NTM experiments showing the effects of EC power and its alignment with the q=2 surface on magnitude of the mode for different NTM control techniques. Shown in the panel from left is the catch and subdue suppression and on the right is the preemptive suppression added results. In the figure magenta color corresponds to fully suppressed modes.

As in the 3/2 case, early mode detection is critical for faster 2/1 "catch and subdue" suppression as shown in figure 12. Islands caught larger than a critical amplitude take much longer to suppress. This critical amplitude for the 2/1 island is found to be approximately 4 Gauss, as once this level is passed, the mode is completely suppressed in a few hundred msec. Cases (not shown) that do not reach the lower critical level do not get stabilized. The 2/1 mode critical level, as for the 3/2 modes, is reached when the island full width is approximately twice that of the ion banana width. Unfortunately, in this case, the mode was never caught below this value due to n=1 noise from sawteeth and ELMs appearing in the Mirnov channels. The island detection threshold had to be kept above 7 Gauss to avoid false positives in the catch and subdue control. Below this value, mode detection algorithm picks up sawteeth signals as 2/1 NTM which leads to gyrotons to turn on when there is no 2/1 NTM. Further reduction in 2/1 NTM suppression power and time with catch and subdue is

predicted for detection below the critical amplitude when the n=1 Mirnov signal is band-pass frequency filtered to have the false positive catch level at or below the critical level for suppression.

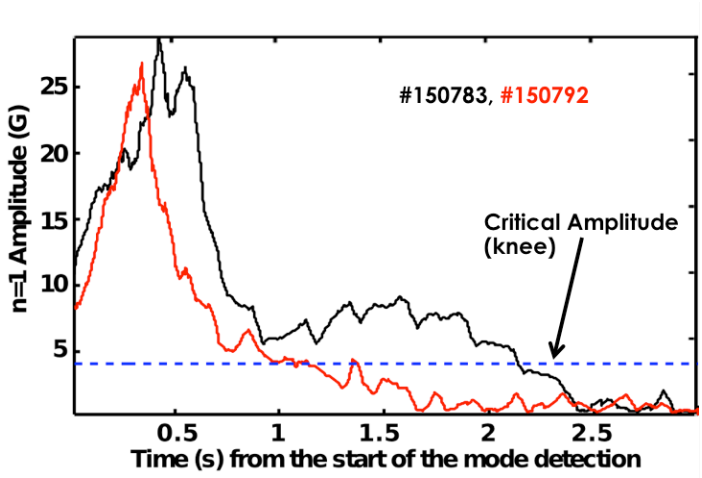

Figure 12. Effect of large initial mode size (larger than the critical level) on 2/1 mode suppression. No cases of small 2/1 initial mode size yet in hand due to n=1 sawteeth and fishbone noise.

5. Conclusion and Future Work

A new integrated real-time NTM control system has been successfully demonstrated on DIII-D. This system consists of multiple real-time elements in the plasma control system: (1) mode detection with Fourier analysis of the Mirnov diagnostics, (2) high accuracy equilibrium reconstruction of rational surface q=m/n locations with MSE, (3) a refraction algorithm using microwave interferometer signals that gives the location of the ECCD based on the mirror positions, (4) automatic mode based control of the on/off of the gyrotron power, (5) fast EC steerable mirrors that are directed to align the ECCD on the rational m/n surface being controlled, and finally (6) the fully automatic control algorithm “catch and subdue” that fuses all the ingredients together.

Remaining work includes the enhancement of the ability to identify all islands below the critical amplitude. For this purpose, a real-time ECE diagnostic is being developed for localizing the Mirnov signals to a specific q surface, as well as a new frequency-enhanced filter being developed that will enable the separation of noise from the sawteeth and ELMs from the NTM signals. Finally, an upgrade to the control algorithm will enable multiple phases of NTM suppression by turning the gyrotrons off after the mode is fully suppressed and turning them back on again when the mode re-emerges.

The DIII-D results show promise in demonstrating how the problem of NTMs can be solved with the least power (peak requirement) and energy (integrated power requirement) from the gyrotron system, thereby maintaining a high Q, by use of these advanced feedback and control techniques. The integrated NTM control developed at DIII-D provides an efficient approach for the control of NTMs in ITER.

Acknowledgements

This work is supported by the US Department of Energy under DE-AC02-09CH11466, DE-FC02-04ER54698, and DE-FG0204ER54761.

References:

[1] R. Prater, “Stabilization and prevention of the 2/1 neoclassical tearing mode for improved performance in DIII-D”, Nuclear Fusion, 47, 371–377 (2007)

[2] R. J. La Haye, “Neoclassical tearing modes and their control”, Physics of Plasmas, 13, 055501 (2006)

[3] D. Humphreys et. al., “Active control for stabilization of neoclassical tearing modes”, Physics of Plasmas, 13, 056113 (2006)

[4] E. Kolemen et. al., “Real-time Mirror Steering for Improved Closed Loop Neoclassical Tearing Mode Suppression by Electron Cyclotron Current Drive in DIII-D”, Fusion Engineering and Design, To appear (2013)

[5] John Lohr, et. al., “The Electron Cyclotron Resonant Heating System on the DIII-D Tokamak”, Fusion Science and Technology, 48, 1226-1237 (2005)

[6] D. Ponce, et. al., “ECH System Developments Including the Design of an Intelligent Fault Processor on the DIII-D Tokamak”, Fusion Engineering and Design, 86, 785 (2011)

[7] R. J. La Haye, “Prospects for stabilization of neoclassical tearing modes by electron cyclotron current drive in ITER”, 49, 045005, (2009)

[8] O Sauter et al., “On the requirements to control neoclassical tearing modes in burning plasmas”, Plasma Phys. Control. Fusion 52 025002 (17pp) (2010)

[9] R.J. La Haye, S. Guenter, D.A. Humphreys, J. Lohr, T.C. Luce, M.E. Maraschek, C.C. Petty, R. Prater, J.T. Scoville, and E.J. Strait, "Control of neoclassical tearing modes in DIII-D," Physics of Plasmas 9, 2051 (2002)

[10] R.J. La Haye, D.A. Humphreys, J.R. Ferron, T.C. Luce, F.W. Perkins, et al, "Higher stable beta by use of pre-emptive electron cyclotron current drive on DIII-D", Nucl. Fusion 45, L37 (2005)

[11] M. Maraschek et al., Phys. Rev. Lett. 93 025005 (2007)

[12] B.A. Hennen et al., Plasma Physics and Controlled Fusion 52, 104006-1/20 (2010).

[13] M. Lennholm M et al., Nucl. Fusion 43, 1458-76 (2003)

[14] A. Isayama et al., Nucl. Fusion 49, 055006 (2009)

[15] A. Isayama et al., Nucl. Fusion 43 (2003) 1272

[16] K. Nagasaki et al., Nucl. Fusion 43 (2003) L7

Figure Captions

Fig 1. Growth of the 2/1 island and the locking of the mode in ITER: On the left: Experimental result from DIII-D with a ITER-like configuration (Shot #148792). On the right: Numerical simulation of the ITER behavior from Ref. [7].

Figure 2. Block diagram of the real-time NTM control system.

Figure 3. Advanced control of the steerable-mirror enables real-time tracking of the NTM. Δz is the difference between the z position of the intersection of the q-surface with the $2f_{ce}$ surface and the average z-position estimated from similar shots.

Figure 4. Suppression of a saturated NTM formation by depositing ECCD (slowly modulated for alignment checkout) at the island location after the mode appears.

Figure 5. a) Experiment with no ECCD, a 3/2 NTM forms and saturates. b) Repeat of the same experiment with pre-emption of NTM formation by depositing ECCD at the island location before the mode appears. "Incidents" at $t \approx 2500$ and 3300 msec. are quickly suppressed automatically.

Figure 6. n=2 amplitude (a proxy for 3/2 island size) and the ECCD power for two shots with and without catch and subdue control. In red: Saturated NTM with no ECCD (Beam drops after 5 sec). In blue: Catch and subdue NTM suppression. The ECCD is turned full on when the mode is detected and the mode is promptly suppressed.

Figure 7. Catch and subdue works well even starting from a deliberate 4 cm misalignment between ECCD and the q surface. *Top:* 3/2 Mode Amplitude. *Top-middle:* Alignment error. *Bottom-middle:* ECH Power. *Bottom:* Contour plot of ECCD current density where black is 0 A/cm^2, blue is 3 A/cm^2, red is 6 A/cm^2, and yellow is 12 A/cm^2. Overlaid in white is the 3/2 surface location and in green is the island size and location.

Figure 8. Overview of the 3/2 NTM experiments showing the effects of EC power and its alignment with the q=3/2 surface on magnitude of the mode for different NTM control techniques. Shown in the panel from left to right are the saturated mode suppression, the catch and subdue suppression added, and finally the preemptive suppression added results. In the panels magenta color corresponds to fully suppressed modes.

Figure 9. Mode amplitude from the start of the NTM detection and ECCD deposition for 3/2 NTM suppression. In red are 2 late "catch" shots and in blue are the 3 early "catch" shots.

Figure 10. Example of 2/1 "catch and subdue" NTM control. *Top:* 2/1 Mode Amplitude. *Bottom:* Contour plot of ECCD current density where black is 0 A/cm^2, blue is 3 A/cm^2, red is 6 A/cm^2, and yellow is 12 A/cm^2. Overlaid in white is the 2/1 surface location and in green is the island size and location.

Figure 11. Contour plot overview of the 2/1 NTM experiments showing the effects of EC power and its alignment with the q=2 surface on magnitude of the mode for different NTM control techniques. Shown in the panel from left is the catch and subdue suppression and on the right is the preemptive suppression added results. In the figure magenta color corresponds to fully suppressed modes.

Figure 12. Effect of large initial mode size (larger than the critical level) on 2/1 mode suppression. No cases of small 2/1 initial mode size yet in hand due to n=1 sawteeth and fishbone noise.

List of Figures

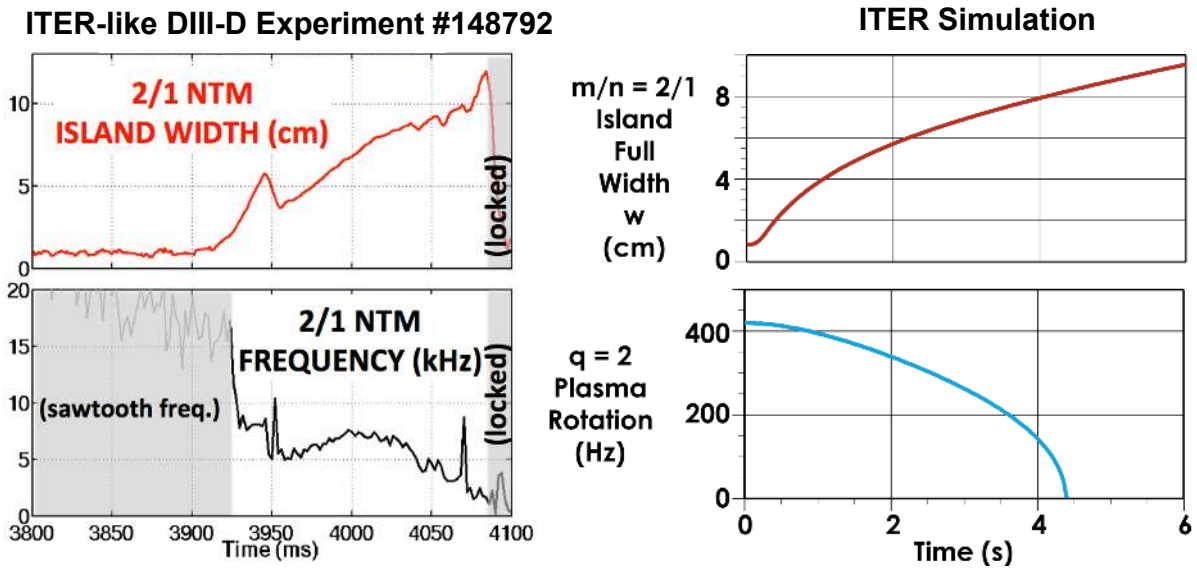

Fig. 1

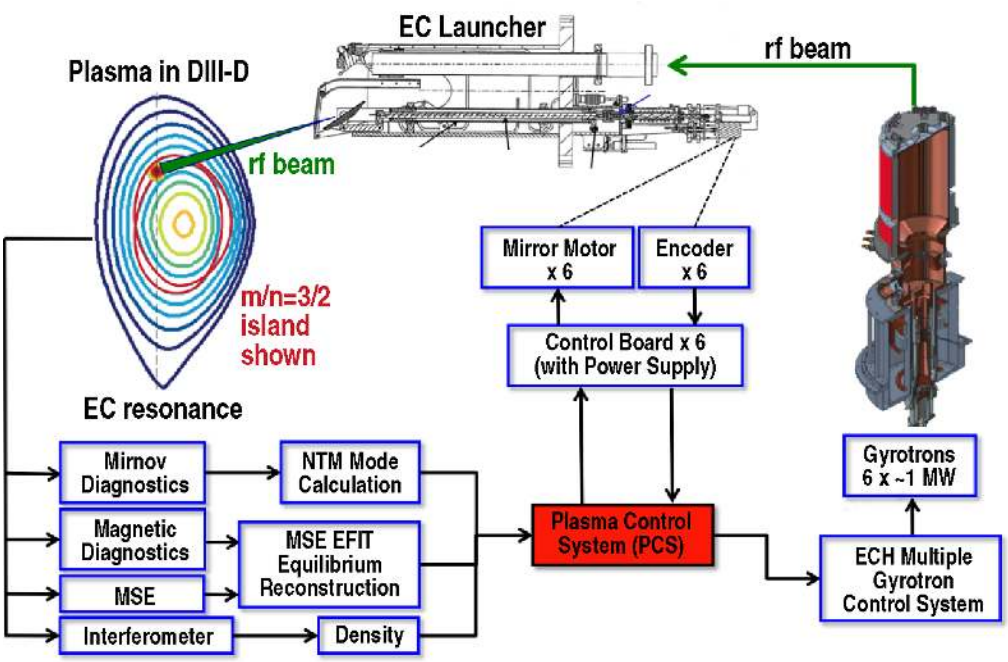

Fig. 2

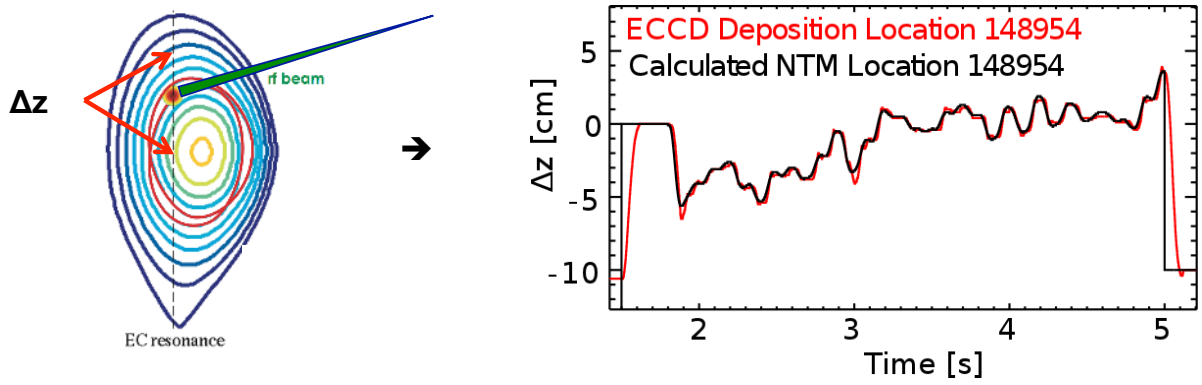
Δz
rf beam
EC resonance
ECCD Deposition Location 148954
Calculated NTM Location 148954
Δz [cm]
Time [s]

Fig. 3

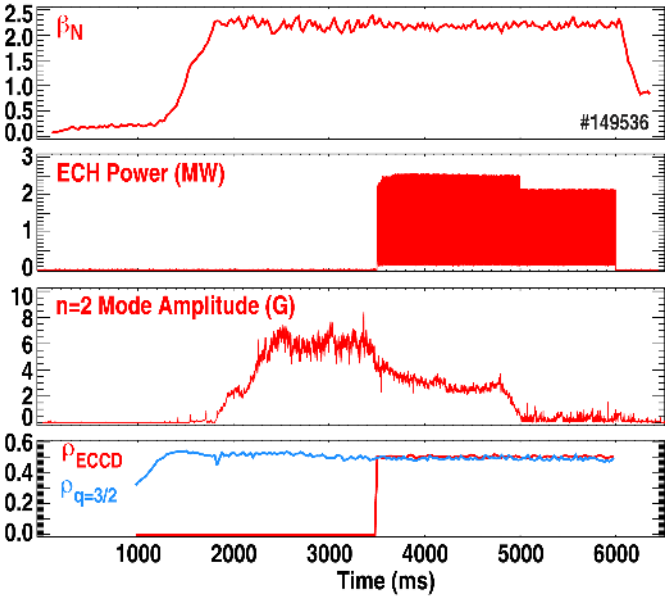
βN
#149536
ECH Power (MW)
n=2 Mode Amplitude (G)
ρECCD
ρq=3/2
Time (ms)

Fig. 4

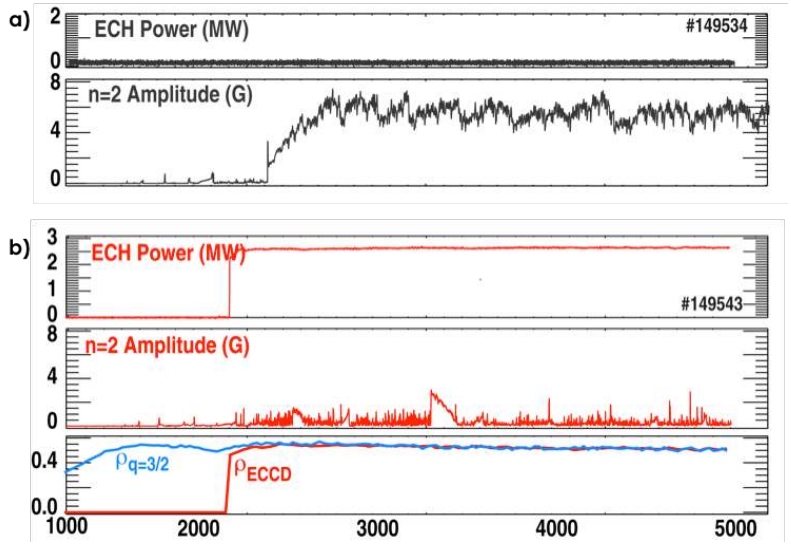
a)
ECH Power (MW)
#149534
n=2 Amplitude (G)
b)
ECH Power (MW)
#149543
n=2 Amplitude (G)
ρq=3/2
ρECCD
1000
2000
3000
4000
5000

Fig 5

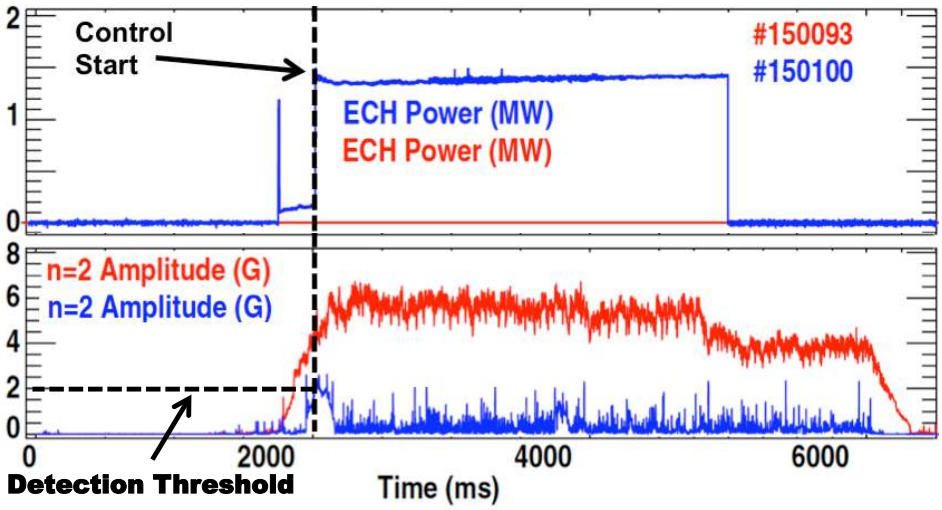
Control
Start
#150093
#150100
ECH Power (MW)
ECH Power (MW)
n=2 Amplitude (G)
n=2 Amplitude (G)
Detection Threshold
Time (ms)

Fig. 6

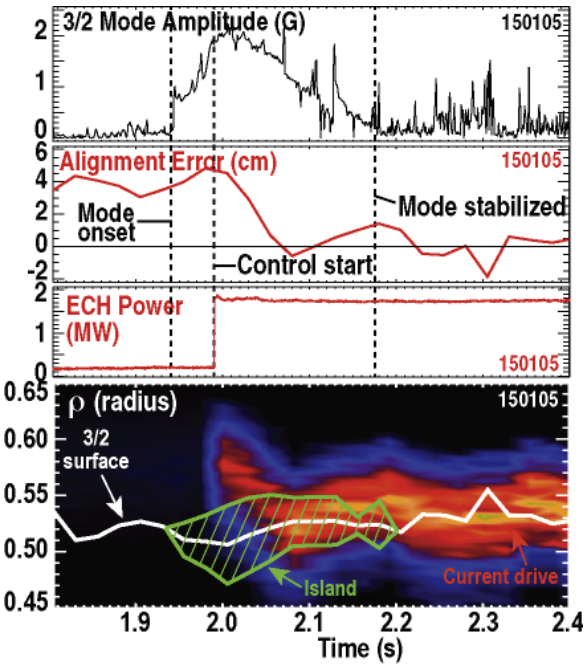
3/2 Mode Amplitude (G)
150105
Alignment Error (cm)
150105
Mode onset
Control start
Mode stabilized
ECH Power (MW)
150105
ρ (radius)
150105
3/2 surface
Island
Current drive
Time (s)

Fig. 7

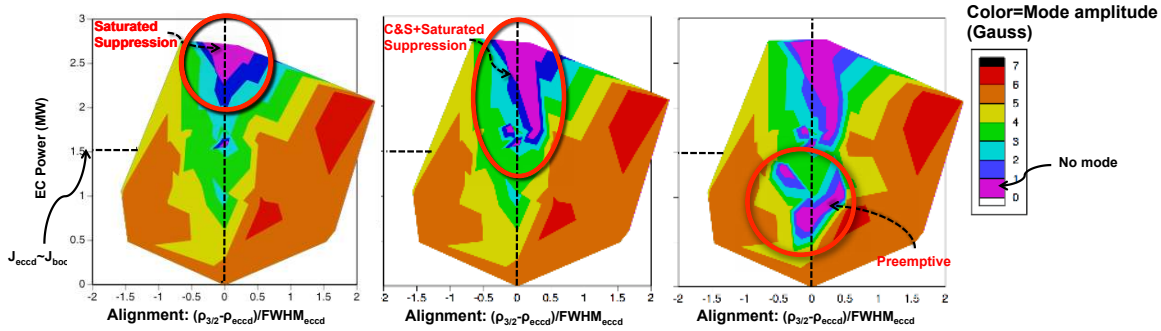

Fig. 8

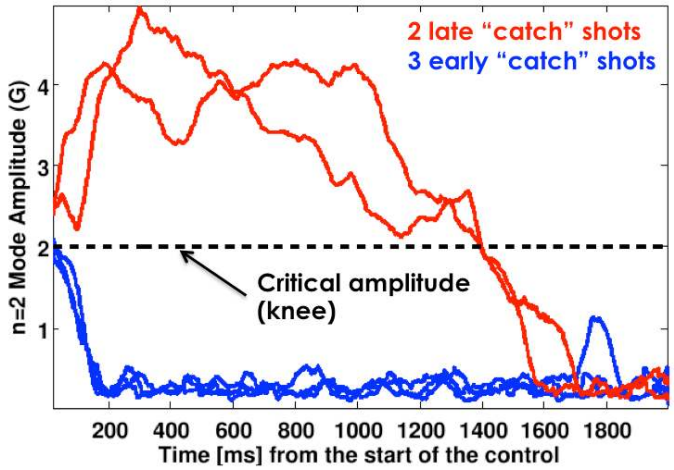

Fig. 9

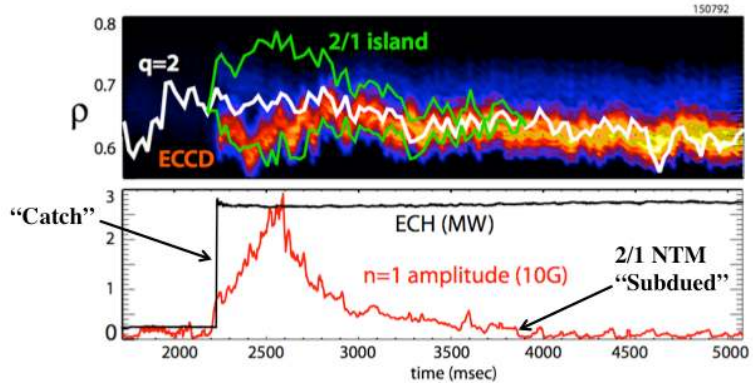

Fig 10

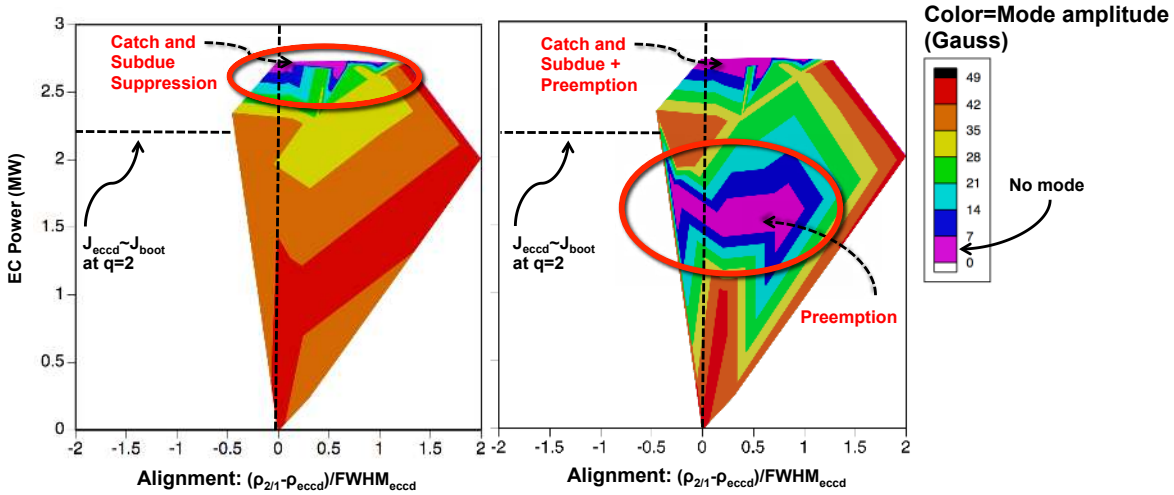
Color=Mode amplitude (Gauss)
49
42
35
28
21
14
7
0
No mode
Catch and Subdue Suppression
Catch and Subdue + Preemption
Preemption
J_{eccd}~J_{boot} at q=2
EC Power (MW)
Alignment: $(\rho_{2/1}-\rho_{eccd})/FWHM_{eccd}$

Fig 11

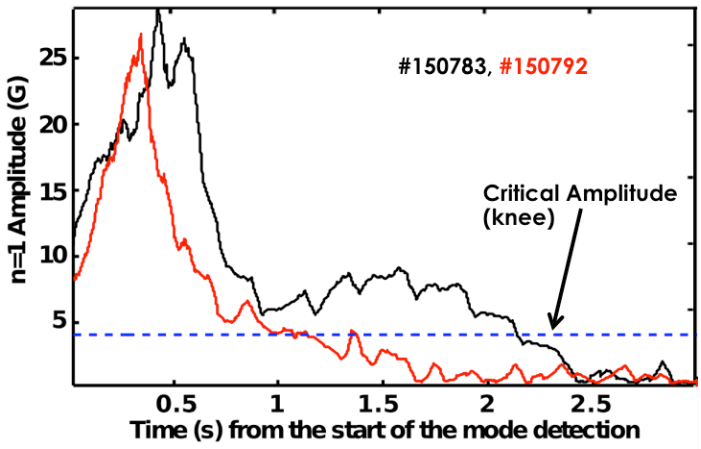
#150783, #150792
Critical Amplitude (knee)
n=1 Amplitude (G)
Time (s) from the start of the mode detection

Fig 12